IMPACT OF NANOPARTICLE ELECTRIFICATION AND VISCOUS DISSIPATION IN THE STAGNATION POINT NANOFLUID FLOW WITH HEAT AND MASS TRANSFER TOWARDS AN EXPONENTIALLY STRETCHING SHEET

Geeta Shivapuji
Government First Grade College Raibag,
Dist. Belagavi, Karnataka.

ABSTRACT:

Nanofluid flows are of major importance in industrial sectors including power generation, transportation, nuclear reactors, thermal therapy for cancer treatment, micro manufacturing, metallurgical and chemical sectors, as well as cooling, heating and air conditioning and also of great economic, social and environmental importance due to their application in many practical fields of science, engineering and technology. Problems concerned with thermal management are some of the areas where the dynamics of nanofluids play a prominent role. Boundary layer flow analysis over some well-known solid surfaces, such as, flat plate, stretching sheet or stretching cylinder problems have a wide range of applications, such as nuclear reactors cooled during an emergency shutdown, electronic devices cooled by fans, gradual cooling of continuous stretched metal or plastic strips, cooling of an infinite metallic plate in a cooling bath, paper production and coating of cylindrical wires.gradual cooling of continuous stretched metal or plastic strips, cooling of an infinite metallic plate in a cooling bath, paper production and coating of cylindrical wires. The literature on the study of boundary layer flow and improvement of heat transfer characteristics of nanofluids scanty and many gaps do exist in the literature. To cite a few the effects of different boundary shapes on the characteristics of flow of nanofluid is still unexplored to the fullest extent. Also the effect of electrification of nanoparticles mechanism has not been attempted in any previous study on modelling of nanofluid flow.
The present investigation is an attempt to study the effect of electrification of nanoparticles mechanism in the modelling of boundary layer flow with heat and mass transfer of a nanofluid. newlineThe pioneering work presented by Choi (1995) suggests that nanofluids can constitute an interesting alternative for advanced applications in heat transfer. Buongiorno (2006) identified multiple mechanisms in the convective transport in nanofluids using a two-phase non-homogeneous model including inertia, Brownian diffusion thermophoresis, diffusiophoresis, the magnus effect, fluid drainage and gravity and he found on

Keywords - Electrification, Heat-Transformation,Mass Transfer, Nanofluids Nanoparticles.

1. INTRODUCTION

The boundary layer flow past an exponentially stretching sheet has been carried out by several researchers. For instance, Magyari and Keller (1999), Nadeem and Lee (2012), Bachok et al. (2012), Malvandi et al.

(2013), Rahman et al. (2014), Bhattacharyya and Layek (2014), Sandeep et al. (2016), Rehman et al. (2018), Alblawi et al. (2019), Narender and Sarma (2019), Wahid et al. (2021) have investigated the boundary layer flow past an exponentially stretching sheet either by considering regular fluid or nanofluid by taking different physical aspects such as viscous dissipation, thermal radiation, chemical reaction, MHD effect and other aspects. So far as boundary layer nanofluid flow towards an exponentially stretching sheet with MHD effect, the base fluid is considered to be electrically conducting and electrification of nanoparticles has not been considered. Despite various works have been presented on nanofluid flow past an exponentially stretching sheet, there seems to be no attempts in literature to consider the effect of nanoparticle electrification on nanofluid flow towards an exponentially stretching sheet where base fluid is electrically non conducting and particles are electrified. So, it is essential to include this mechanism in nanofluid flow towards an exponentially stretching sheet problem.

This chapter presents the influence of thermophoresis, nanoparticle electrification, viscous dissipation and Brownian motion on the stagnation point flow with heat and mass transfer of a nanofluid towards an exponentially stretching sheet.

2. ANALYSIS OF THE PROBLEM

Consider a laminar steady incompressible two dimensional boundary layer flow of a Cu-Water nanofluid with electrification of nanoparticles near the stagnation point at a stretching sheet as shown in Figure -1. The cartesian coordinate system is taken with the origin at the stagnation point. The x-axis is taken along the stretching sheet and the y axis is perpendicular to the plane of the sheet. The flow takes place in the region $y > 0$.On both sides of the stretching sheet, two opposite forces are applied such that the sheet is stretched while the origin remains fixed. The ambient fluid velocity $U_e(x) = ae^{x/L}$ and the stretching velocity $U_w(x) = be^{x/L}$ are vary nonlinearly, where a and b are positive constants and L is the characteristic length. It is considered that the concentration and temperature have constant values at the wall, C_w and T_w respectively, while the ambient concentration and temperature are C_∞ and T_∞ respectively.

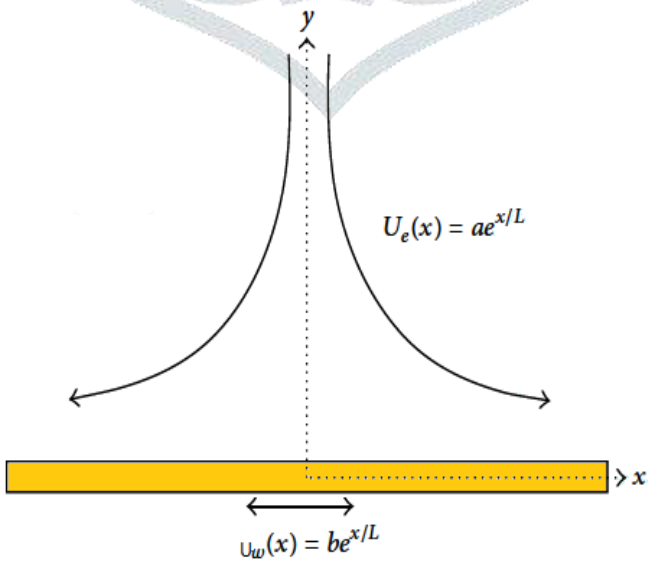

Fig. 1: Physical model and co-ordinate system

The boundary layer equations of continuity, momentum, energy and concentration are expressed as follows [Ref: Appendix-IV]

$$\frac{\partial u}{\partial x}+\frac{\partial v}{\partial y}=0 \tag{1}$$

$$u\frac{\partial u}{\partial x}+v\frac{\partial u}{\partial y}=U_e\frac{\partial U_e}{\partial x}+v_{nf}\frac{\partial^2 u}{\partial y^2}+\frac{\rho_s}{\rho_{nf}}\left(\frac{q}{m}\right)(C-C_\infty)E_x \tag{2}$$

$$(\rho c)_{nf}\left[u\frac{\partial T}{\partial x}+v\frac{\partial T}{\partial y}\right]=k_{nf}\left[\frac{\partial^2 T}{\partial y^2}\right]+(\rho c)_s D_B\frac{\partial C}{\partial y}\frac{\partial T}{\partial y}+\frac{(\rho c)_s D_T}{T_\infty}\left(\frac{\partial T}{\partial y}\right)^2$$
$$+\left(\frac{q}{m}\right)\frac{(\rho c)_s C}{F}\left(E_x\frac{\partial T}{\partial x}+E_y\frac{\partial T}{\partial y}\right)+\mu_{nf}\left(\frac{\partial u}{\partial y}\right)^2 \tag{3}$$

$$u\frac{\partial C}{\partial x}+v\frac{\partial C}{\partial y}=D_B\frac{\partial^2 C}{\partial y^2}+\frac{D_T}{T_\infty}\frac{\partial^2 T}{\partial y^2}+\left(\frac{q}{m}\right)\frac{1}{F}\left[\frac{\partial(CE_x)}{\partial x}+\frac{\partial(CE_y)}{\partial y}\right] \tag{4}$$

Subject to the boundary conditions:

$$\left.\begin{aligned}u=U_w=be^{x/L},v=0,T=T_w,C=C_w \text{ at } y=0\\ u=U_e=ae^{x/L},T=T_\infty,C=C_\infty \text{ as } y\to\infty\end{aligned}\right\} \tag{5}$$

Introducing the stream function ψ with $u=\frac{\partial\psi}{\partial y},v=-\frac{\partial\psi}{\partial x}$ and the nondimensional similarity variables

$$\eta=y\sqrt{\frac{b}{2v_fL}}e^{x/2L},\psi=\sqrt{2bv_fL}e^{x/2L}f(\eta),\theta(\eta)=\frac{T-T_\infty}{T_w-T_\infty},s(\eta)=\frac{c-C_\infty}{C_w-C_\infty} \tag{6}$$

into the equations (1) to (4) and boundary conditions (5).

The continuity equation (1) is thus identically satisfied and the equations (2) to (4) are transferred to the following dimensionless ordinary differential equations.

$$f'''+\varphi_1 ff''+2\varphi_1(\varepsilon^2-f'^2)+2\varphi_1\varphi_2 Sc\frac{MNb}{N_F}s=0 \tag{7}$$

$$\theta''+\frac{Pr}{\varphi_3\varphi_4}f\theta'+\frac{Pr}{\varphi_4}\left[Nbs'\theta'+Nt(\theta')^2+ScNb\left(2\frac{N_F}{N_{Re}}+M\right)(s+Nc)\eta\theta'+\right.$$
$$\left.\varphi_5 Ecf''^2\right]=0 \tag{8}$$

$$s''+Scfs'+\frac{Nt}{Nb}\theta''+MSc\eta s'+2\frac{ScN_F}{N_{Re}}(\eta s'+s+Nc)=0 \tag{9}$$

The dimensionless boundary conditions are

$$\left.\begin{aligned}\eta=0,f=0,f'=1,\theta=1,s=1\\ \eta\to\infty,f'=\varepsilon,\theta=0,s=0\end{aligned}\right\} \tag{10}$$

Here prime denotes derivative with respect to η. The non-dimensional parameters are defined as

$$Sc=\frac{v_f}{D_B},\Pr=\frac{v_f}{\alpha_f},Nb=\frac{(\rho c)_s D_B(C_w-C_\infty)}{(\rho c)_f v_f},Nt=\frac{(\rho c)_s D_T(T_w-T_\infty)}{(\rho c)_f v_f T_\infty},\frac{1}{N_{Re}}=\left(\frac{q}{m}\right)^2\frac{\rho_s L^2}{(U_w)^2\epsilon_0'}$$
$$N_F=\frac{U_w}{FL},M=\left(\frac{q}{m}\right)\frac{1}{FU_w}E_x,\varepsilon=\frac{a}{b},Nc=\frac{C_\infty}{C_w-C_\infty},Ec=\frac{(U_w)^2}{C_f(T_w-T_\infty)}.$$

And the thermophysical constants (Maharukh et al., 2016 and Chavda, 2015) are defined as follows:

$$\varphi_1 = \frac{v_f}{v_{nf}} = \frac{\mu_f}{\mu_{nf}}\frac{\rho_{nf}}{\rho_f} = (1-C_\infty)^{2.5}\left[C_\infty\frac{\rho_s}{\rho_f} + (1-C_\infty)\right],$$

$$\varphi_2 = \frac{c_f}{c_s}\left[\frac{1}{\left[C_\infty\frac{\rho_s}{\rho_f} + (1-C_\infty)\right]}\right],$$

$$\varphi_4 = \frac{k_{nf}}{k_f} = \frac{k_s + 2k_f - 2C_\infty(k_f - k_s)}{k_s + 2k_f + C_\infty(k_f - k_s)}$$

$$\varphi_5 = \frac{\mu_{nf}}{\mu_f} = \frac{1}{(1-C_\infty)^{2.5}}$$

3. METHOD OF SOLUTION

The non-linear ODEs (7) to (9) under the boundary conditions have been solved numerically using MATLABbvp4c solver.

4. TRANSLATION OF DIFFERENTIAL EQUATIONS

The governing equations of the flow field are reduced to O.D.E. are given by:

$$f''' = -\varphi_1 f f'' - 2\varphi_1(\varepsilon^2 - f'^2) - 2\varphi_1\varphi_2\frac{MScNb}{N_F}s$$

$$\theta'' = -\frac{Pr}{\varphi_3\varphi_4}f\theta' - \frac{Pr}{\varphi_4}\left[Nbs'\theta' + Nt(\theta')^2 + ScNb\left(2\frac{N_F}{N_{Re}} + M\right)(s+Nc)\eta\theta' + \varphi_5 Ecf''^2\right]$$

$$s'' = -Scfs' - \frac{Nt}{Nb}\theta'' - MSc\eta s' - 2\frac{N_F Sc}{N_{Re}}(\eta s' + s + Nc)$$

Subjected to the boundary condition

$$\left.\begin{array}{l}\eta = 0, f = 0, f' = 1, \theta = 1, s = 1\\ \eta \to \infty, f' = \varepsilon, \theta = 0, s = 0\end{array}\right\}$$

Let

$$f = f(1)$$
$$f' = f(2), f(0) = 0 \text{ or } f_0(1) = 0$$
$$f'' = f(3), f'(0) = 1 \text{ or } f_0(2) = 1$$
$$f''' = -\varphi_1 f f'' - 2\varphi_1\left(\varepsilon_s{}^2 - f'^{2^2}\right) - 2\varphi_1\varphi_2\frac{MScNb}{N_F}s$$

$$\text{Or } f''' = -\varphi_1 f(1)f(3) - 2\varphi_1(\varepsilon^2 - (f(2))^2) - 2\varphi_1\varphi_2 \frac{MScNb}{N_F} f(6), f''(0) =$$

$$\text{unknown, } f_{inf}(2) = \varepsilon$$

$$\theta = f(4)$$

$$\theta' = f(5), \theta(0) = 1 \text{Or } f_0(4) = 1$$

$$\theta'' = -\frac{Pr}{\varphi_3\varphi_4} f\theta' - \frac{Pr}{\varphi_4}\left[Nbs'\theta' + Nt(\theta')^2 + ScNb\left(2\frac{N_F}{N_{Re}} + M\right)(s + Nc)\eta\theta' + \varphi_5 Ecf''^2\right],$$

$$\text{or } \theta'' = -\frac{Pr}{\varphi_3\varphi_4} f(1)f(5) - \frac{Pr}{\varphi_4}\left[Nbf(7)f(5) + Nt(f(5))^2 + ScNb\left(2\frac{N_F}{N_{Re}} + M\right)(f(6) + Nc)\eta f(5) + \varphi_5 Ec(f(3))^2\right], \theta'(0) = \text{ unknown, } f_{\text{inf}}(4) = 0$$

$$s = f(6)$$

$$s' = f(7), \text{s}(0) = 1 \text{ Or } f_0(6) = 1$$

$$s'' = -Scfs' - \frac{Nt}{Nb}\theta'' - MSc\eta s' - 2\frac{N_F Sc}{N_{Re}}(\eta s' + s + Nc)$$

Or

$$s'' = -\text{Sc} f(1)f(7) - \frac{Nt}{Nb}\theta'' - MSc\,\eta f(7) - 2\frac{N_F Sc}{N_{Re}}(\eta f(7) + f(6) + Nc),$$

$$s'(0) = \text{ unknown }, f_{\text{inf}}(6) = 0$$

5. CALCULATION OF SHERWOOD NUMBER, NUSSELT NUMBER AND SKIN FRICTION COEFFICIENT

The local Sherwood number Sh_x, local Nusselt number Nu_x and skin friction coefficient C_f which are defined as

$$Sh_x = \frac{xq_m}{D_B(C_w - C_\infty)}, Nu_x = \frac{xq_w}{k_f(T_f - T_\infty)'}\ C_f = \frac{\tau_w}{\rho_f U_w^2}$$

where, $\tau_w = \mu_f \left(\frac{\partial u}{\partial y}\right)_{y=0}$ is the wall shear stress, $q_w = -k_f \left(\frac{\partial T}{\partial y}\right)_{y=0}$ is the local heat flux and $q_m = -D_B \left(\frac{\partial C}{\partial y}\right)_{y=0}$ is the local mass flux.

Using

$$\frac{\partial u}{\partial y} = be^{3x/2L}\sqrt{\frac{b}{2v_f L}}f'', \frac{\partial T}{\partial y} = \sqrt{\frac{b}{2v_f L}}e^{x/2L}(T_w - T_\infty)\theta', \frac{\partial C}{\partial y} = \sqrt{\frac{b}{2v_f L}}e^{x/2L}(C_w - C_\infty)s'$$

We get

$$\tau_w = \mu_f be^{3x/2L}\sqrt{\frac{b}{2v_f L}}f''(0), q_w = -k_f\sqrt{\frac{b}{2v_f L}}e^{x/2L}(T_w - T_\infty)\theta'(0), q_m =$$

$$-D_B\sqrt{\frac{b}{2v_f L}}e^{x/2L}(C_w - C_\infty)s'(0)$$

$$C_f = \frac{\mu_f be^{3x/2L}\sqrt{\frac{b}{2v_f L}}}{\rho_f(be^{x/L})^2}f''(0) = e^{-x/2L}\sqrt{\frac{v_f}{2bL}}f''(0) = \sqrt{\frac{v_f}{2be^{x/L}}}f''(0) = \sqrt{\frac{v_f}{2U_w x}}\sqrt{\frac{x}{L}}f''(0)$$

$$= (2Re_x)^{-1/2}\sqrt{\frac{x}{L}}f''(0)$$

$$\Rightarrow C_f(2Re_x)^{1/2}\sqrt{\frac{L}{x}} = f''(0)$$

$$Nu_x = -\frac{xk_f\sqrt{\frac{b}{2v_f L}}e^{x/2L}(T_w - T_\infty)}{k_f(T_w - T_\infty)}\theta'(0) = -\sqrt{\frac{be^{x/L}x}{2v_f}}\sqrt{\frac{x}{L}}\theta'(0) = -\sqrt{\frac{U_w x}{2v_f}}\sqrt{\frac{x}{L}}\theta'(0)$$

$$= -\left(\frac{Re_x}{2}\right)^{\frac{1}{2}}\sqrt{\frac{x}{L}}\theta'(0)$$

$$\Rightarrow Nu_x(Re_x/2)^{-1/2}\sqrt{\frac{L}{x}} = -\theta'(0)$$

$$Sh_x = -\frac{xD_B\sqrt{\frac{b}{2v_fL}}e^{x/2L}(C_w - C_\infty)s'(0)}{D_B(C_w - C_\infty)} = -\sqrt{\frac{be^{x/L}x}{2v_f}}\sqrt{\frac{x}{L}}s'(0) = -\sqrt{\frac{U_w x}{2v_f}}\sqrt{\frac{x}{L}}s'(0)$$

$$= -\left(\frac{Re_x}{2}\right)^{\frac{1}{2}}\sqrt{\frac{x}{L}}s'(0)$$

$$\Rightarrow Sh_x(Re_x/2)^{-1/2}\sqrt{\frac{L}{x}} = -s'(0)$$

In dimensionless form the reduced Sherwood number $(-s'(0))$, reduced Nusselt number $(-\theta'(0))$ and reduced skin friction coefficient $(f''(0))$ can be written as:

$$Sh_x(Re_x/2)^{-1/2}\sqrt{\frac{L}{x}} = -s'(0)$$

$$Nu_x(Re_x/2)^{-1/2}\sqrt{\frac{L}{x}} = -\theta'(0)$$

$$C_f(2Re_x)^{1/2}\sqrt{\frac{L}{x}} = f''(0)$$

where $Re_x = \frac{U_w x}{v_f}$ is the local Reynolds number.

6. DISCUSSION OF RESULTS

In this problem the nanofluid is water based with Pr = 6.2 (considering pure water) containing 1% of copper (Cu) nanoparticle. The thermophysical characteristics (Oztop and Abu-Nada, 2008) of the Cu - water nanofluid are shown in Table 1.

Table 1: Thermophysical characteristics

Property	Fluid(Pure water)	Solid(Cu)
$c_p(J/\text{kgK})$	4162	378
$\rho(\text{kg/m}^3)$	990.1	8833
$k(\text{W/mK})$	0.603	398
$\beta \times 10^{-5}(1/\text{K})$	22	1.65

Numerical solutions are obtained for the effects of Brownian motion, thermophoresis, viscous dissipation and electrification of nanoparticles on heat and mass transfer in stagnation point flow of the Cu -Water nanofluid toward an exponentially stretching sheet. To ensure that the numerical computations are accurate, the values of $f''(0)$ and $f(\infty)$ are compared with the results computed by Magyari and Keller (1999) in

Table 2 for regular fluid (absence of nanoparticles) without viscous dissipation and it is found to be an excellent agreement.

Table 2: The comparison of values of $f''(0)$ and $f(\infty)$

	Magyari and Keller (1999)	Present results
$-f''(0)$	1.271254	1.27192
$f(\infty)$	0.915649	0.91545

The distributions of dimensionless longitudinal velocity $\frac{df(\eta)}{d\eta}$, temperature $\theta(\eta)$ and nanoparticle concentration $s(\eta$ are depicted in Fig. 2.

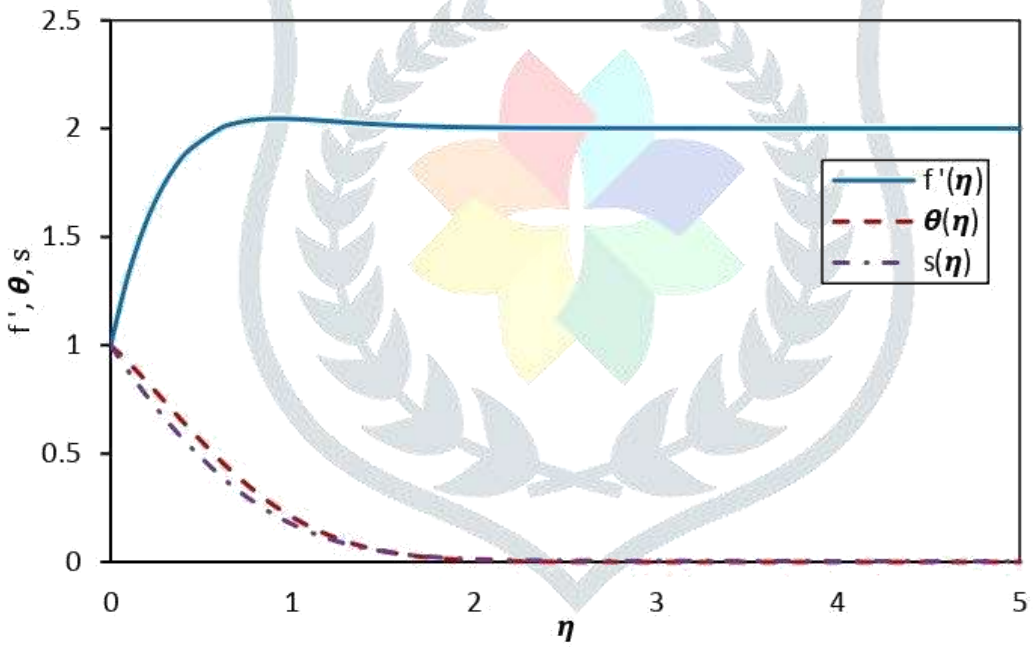

Fig. 2: Plots of dimensionless similarity functions $\frac{df(\eta)}{d\eta}, \theta(\eta)$ and $s(\eta)$ for the case

$$Sc = 2.0, Nb = Nt = M = Ec = Nc = N_F = 0.1, \varepsilon = 2.0, N_{Re} = 2.0, \Pr = 6.2$$

The results obtained show the effects of thermophoresis parameter Nt, Brownian motion parameter Nb, electrification parameter M, stretching parameter ε and Eckert number Ec on the velocity profile $f'(\eta)$, temperature profile $\theta(\eta)$, concentration profile $s(\eta)$. Also the effect of these parameters on $f''(0), -\theta'(0)$ and $-s'(0)$ is presented in tabular form.

6. VELOCITY PROFILES

The vertical component of the velocity profiles are depicted in Figures 3 to 6. Figures 3,4,5 and 6 are presented to examine the effects of Nb, Nt, M, ε and Ec on $f'(\eta)$. Both Figs. 3 and 4 indicate that increasing Nb and Nt are to increase the velocity profile. In particular, the collision of the nanoparticles with the fluid particle increases with the increase of Nb. This phenomenon leads to increase the velocity profile. $f'(\eta)$ increases with Nt due to the increase of the movement of nanoparticles. The combined effects of electrification parameter M and stretching parameter ε on $f'(\eta)$ are examined in Fig. 6.5. The figure reveals that $f'(\eta)$ increases with increasing values of M in both the cases $\varepsilon = 1.0$ (i.e. $a = b$) and $\varepsilon = 2.0$ (i.e. $a \neq b$). In fact, an increase in M implies the increase of drag force on the ions has an equal and opposite reaction force acting on the neutral fluid molecules and consequently the velocity profile increases. When $\varepsilon = 1.0$, there is no change in velocity profile in the absence of electrification parameter M whereas the velocity graphs boost with the presence of electrification parameter M, this indicate that the velocity graph is only influenced by the electrification parameter. This is due to the fact that when $\varepsilon = 1.0$, the stretching velocity $be^{x/L}$ of the surface is equal to the velocity $ae^{x/L}$ of the free stream whereas the electrification phenomenon helps to increase the velocity. It is also noted that $f'(\eta)$ increases with increasing and it is obvious as $f'(\infty)$.

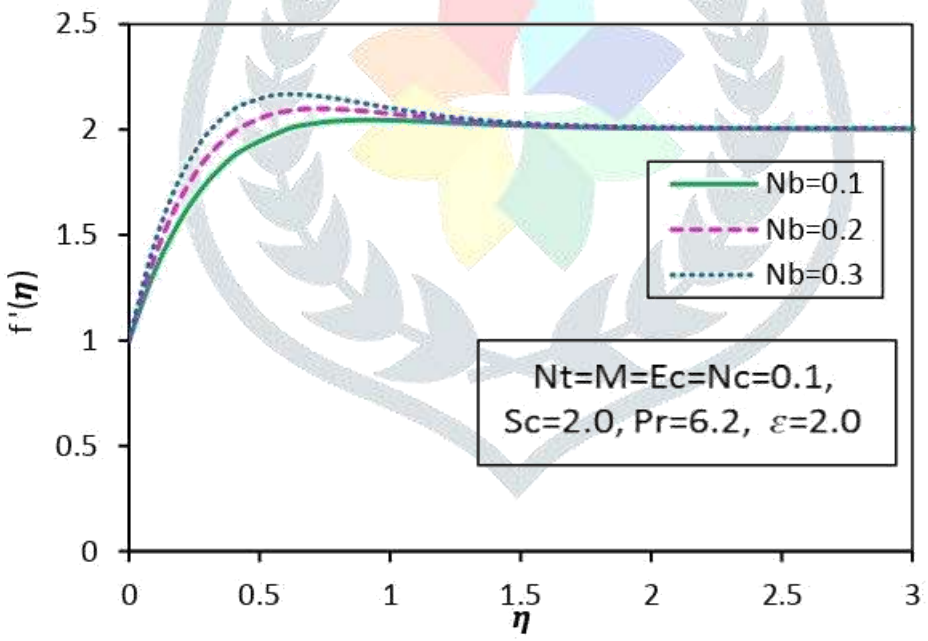

Fig. 3: Variation of $f'(\eta)$ with Nb when $N_{Re} = 2.0, N_F = 0.1$.

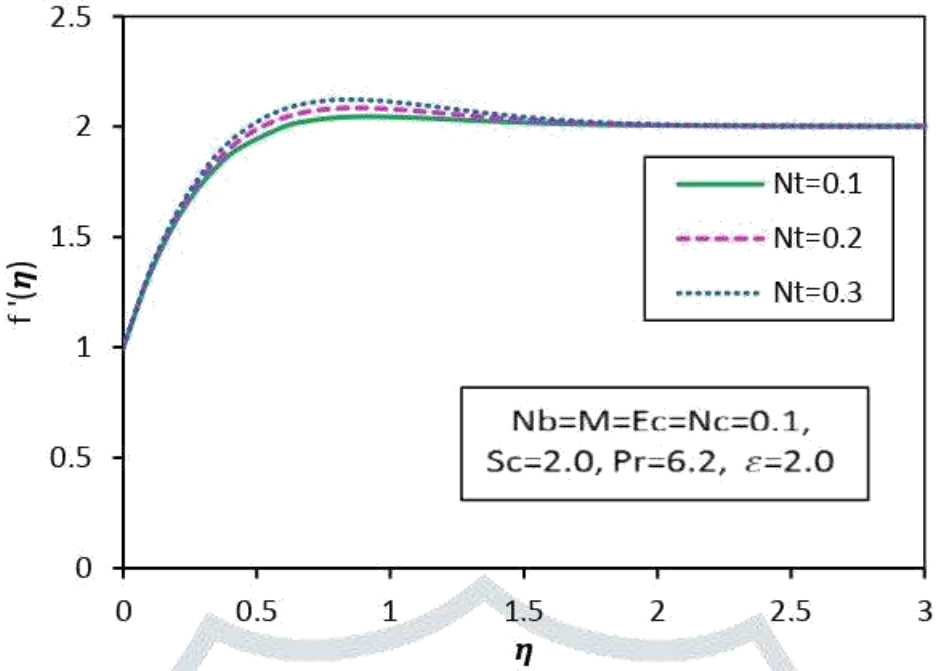

Fig. 4: Variation of $f'(\eta)$ with Nt when $N_{Re} = 2.0, N_F = 0.1$.

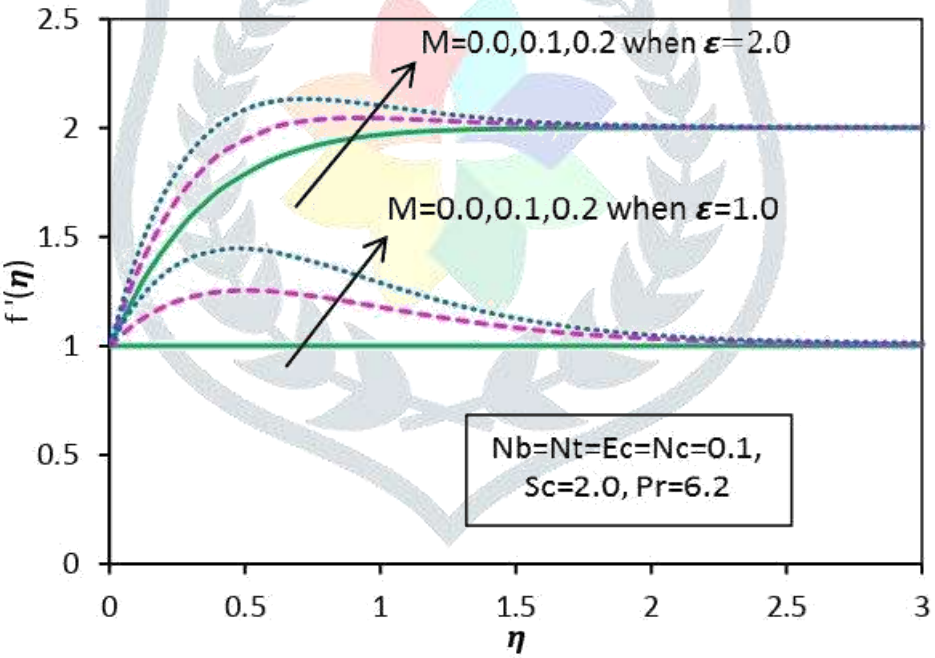

Fig. 5: Variation of $f'(\eta)$ with M when $N_{Re} = 2.0, N_F = 0.1$.

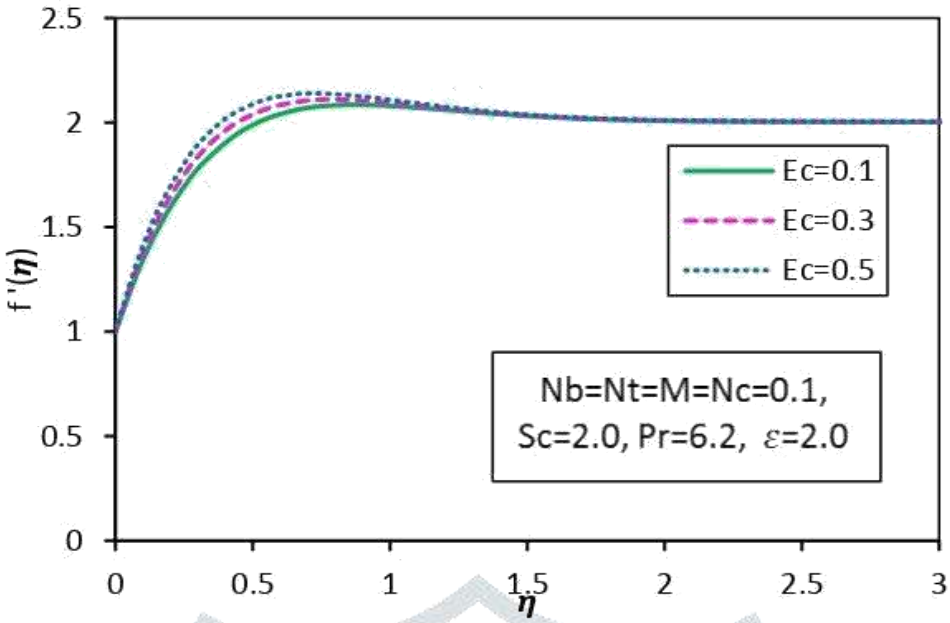

Fig. 6: Variation of $f'(\eta)$ with E_c when $N_{Re} = 2.0, N_F = 0.1$.

CONCENTRATION PROFILES

Figures $7, 8, 9$ and 10 are plotted to demonstrate the effects of Nb, Nt, M, ε and Ec on the concentration profile $s(\eta)$. Fig.7 elucidate that $s(\eta)$ reduces with increasing Nb. Fig.8 indicate that the concentration profile increases when Nt increase. From Fig.9 it is noticed that $s(\eta)$ decreases with increase in M when $\varepsilon = 1.0$ (i.e. $a = b$) and $\varepsilon = 2.0$ (i.e. $a \neq b$). The concentration profile decreases in both the cases because of the movement of nanoparticles increases from fluid region towards the sheet surface when electrification parameter M increases. It is also noted from Fig.9 that both $s(\eta)$ and the concentration boundary layer thickness reduces with ε. Fig.10 reveals that the reduction in concentration profile near the sheet surface is noticed, while the reverse manner is observed far away from the sheet surface with an increase in Ec. This is due to the dominance of conduction near the sheet surface than the convection.

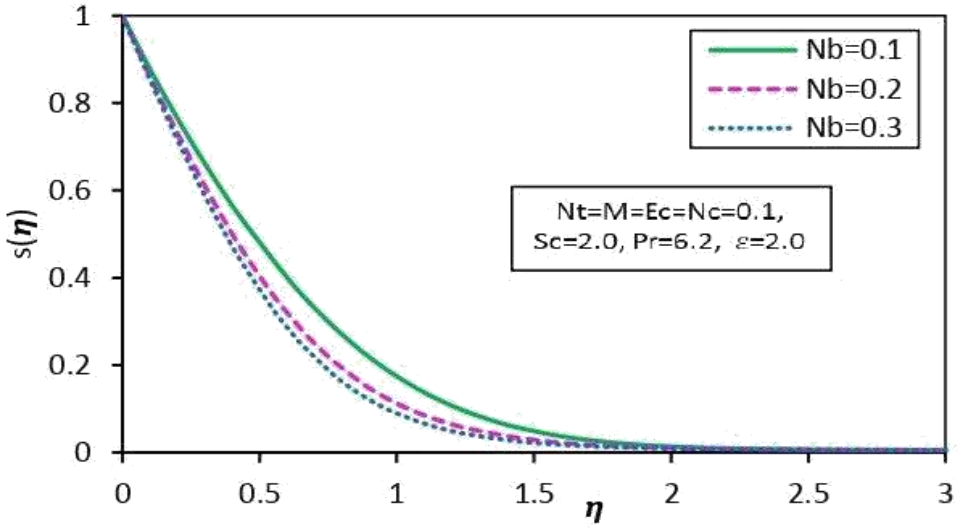

Fig. 7: Variation of S(η) with Nb when $N_{Re} = 2.0, N_F = 0.1$.

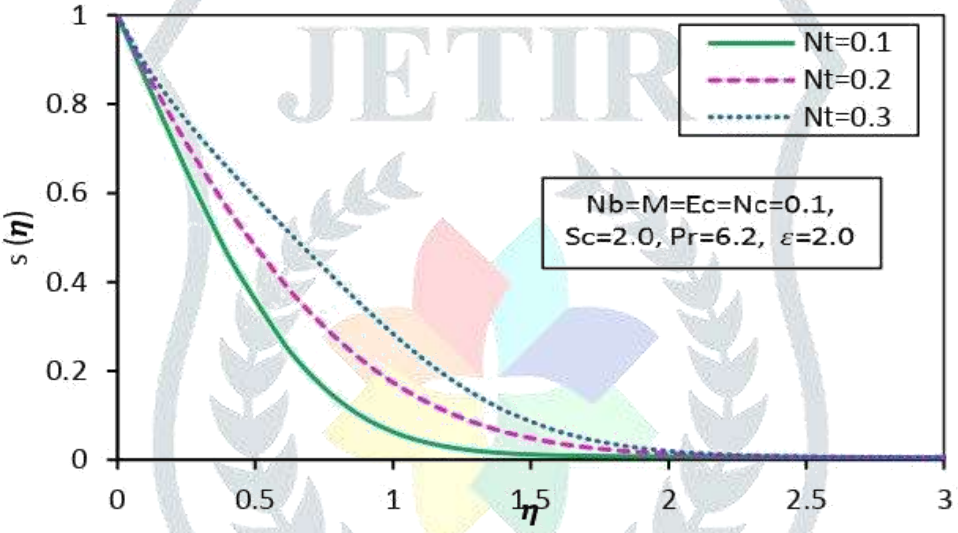

Fig. 8: Variation of S(η) with Nt when $N_{Re} = 2.0, N_F = 0.1$.

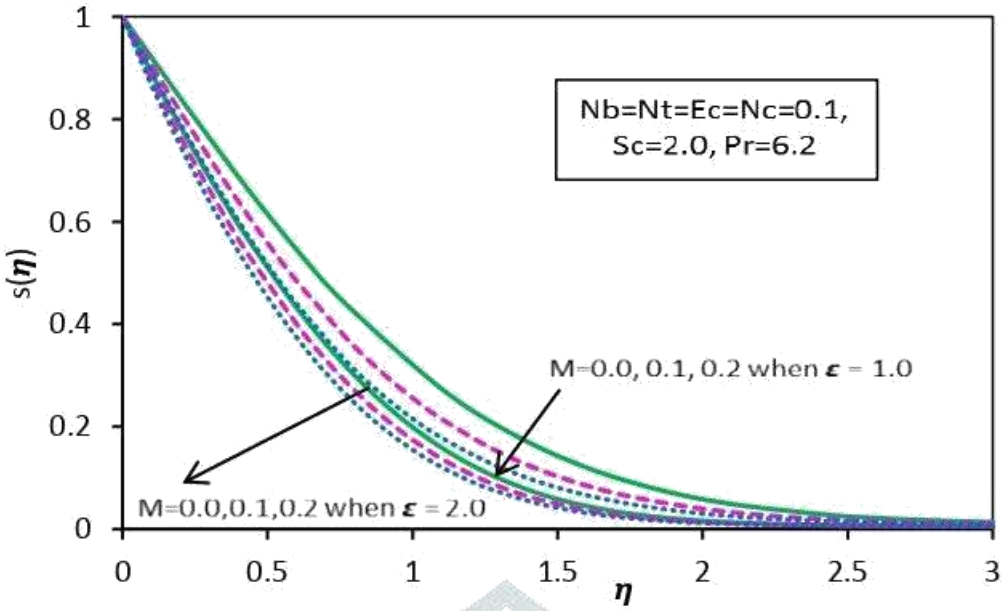

Fig. 9: Variation of $S(\eta)$ with M when $N_{Re} = 2.0, N_F = 0.1$

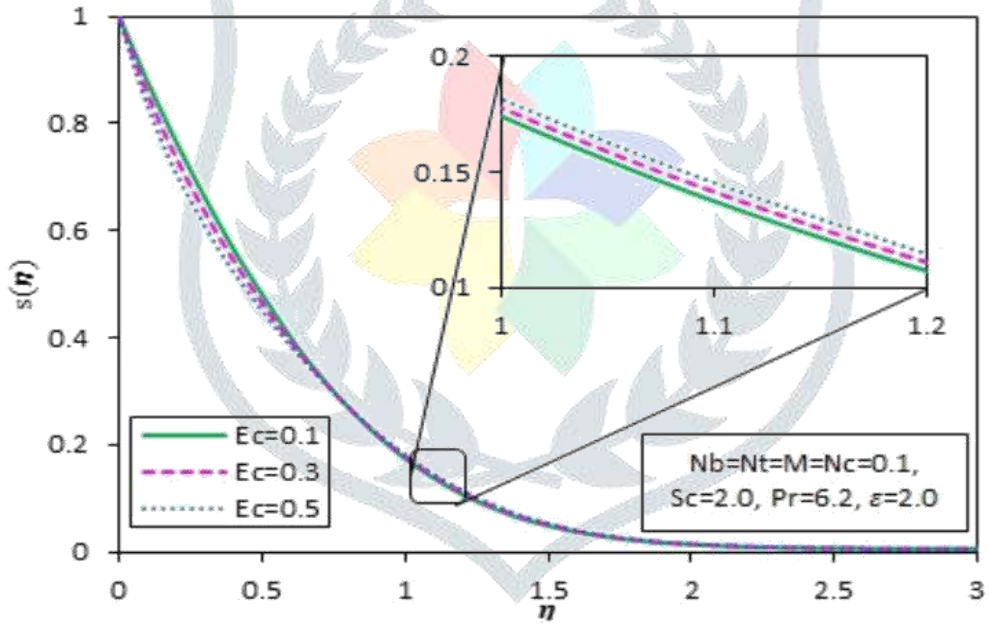

Fig. 10: Variation of S(η) with Ec when $N_{Re} = 2.0, N_F = 0.1$

Dimensionless Skin Friction, Heat and Mass Transfer Coefficients :

Table 3 represents the variation of $f''(0), -\theta'(0)$ and $-s'(0)$ with respect to Nb, Nt and Ec. From Table 3 it is noticed that the $f''(0)$ increases with increasing Brownian motion parameter Nb, thermophoresis parameter Nt and Eckert number Ec. This happens because of the increase of velocity profile at the sheet surface with increasing Nb, Nt and Ec. The reduced Nusselt number $(-\theta'(0))$ decreases with increasing Nb, Nt and Ec. This is due to the enhancement of temperature profile at the sheet surface with increase in Nb, Nt and Ec. $-s'(0)$ increases with increase in Nb and Ec but reduces with increase in thermophoresis parameter Nt. This observation of $-s'(0)$ occurs due to the decrease in $s(\eta)$ with an increase in Nb and Ec whereas the increase in $s(\eta)$ with increasing Nt.

Table 4 is computed to demonstrate the combined effects of M and ε on $f''(0)$, $-\theta'(0)$ and $-s'(0)$. From Table 4 it is reported that the $f''(0)$ increases with increasing M for both the cases $\varepsilon = 1.0$ (i.e. $a = b$) and $\varepsilon = 2.0$ (i.e. $a \neq b$) because increase of velocity profile at the sheet surface with increase in M for both the cases. It is also noticed that the reduced $f''(0)$ increases as stretching parameter ε increases for varied values of M. This is because of the increase of velocity profile at the sheet surface with increasing ε for all the values of M. When $\varepsilon = 1.0$ and $M = 0.0$, then $f''(0)$ is equal to zero as there is no change in velocity distribution while the $f''(0)$ increases in the presence of M because of the increase in velocity distribution. This observation clearly shows that M has a pronounced effect on $f''(0)$. The increase in electrification parameter M helps in increasing the reduced Nusselt number $(-\theta'(0))$ when $\varepsilon = 1.0$ (i.e. $a = b$) whereas helps in decreasing the reduced Nusselt number $(-\theta'(0))$ when $\varepsilon = 2.0$ (i.e. $a \neq b$). This is probably due to the fact that dimensionless surface temperature decreases when $\varepsilon = 1.0$ whereas it increases when $\varepsilon = 2.0$ as M increases. Increasing $\varepsilon, -\theta'(0)$ increases for different values of M. It is worth mentioning that in all Figures 3 to 10 plotted in the problem, the dimensionless temperature, velocity and concentration profiles satisfy the far field boundary conditions (10) asymptotically, demonstrating the correctness of the numerical results presented in the problem.

Table 3: Variation of $f''(0), -\theta'(0)$ and $-s'(0)$ with Nb, Nt and Ec when $M = 0.1, \varepsilon = 2.0, Sc = 2.0, N_{Re} = 2.0, N_F = 0.1, \Pr = 6.2, Nc = 0.1$

Nb	Nt	Ec	$f''(0)$	$-\theta'(0)$	$-s'(0)$
0.1	**0.1**	**0.1**	**3.71957**	**0.73567**	**1.27811**
0.2			4.71362	0.63735	1.43223
0.3			5.56013	0.53236	1.50234
0.1	**0.1**		**3.83957**	**0.74337**	**1.28511**
	0.2		3.90921	0.69237	1.22972
	0.3		3.98722	0.65288	1.16425
	0.1	**0.1**	**3.88757**	**0.73337**	**1.27611**
		0.3	3.88214	0.34899	1.64332
		0.5	3.96606	0.02813	1.97269

Table 4: The effects of ε and M on $f''(0), -\theta'(0)$ and $-s'(0)$ when $Nb = 0.1, Nt = 0.1, Ec = 0.1, Sc = 2.0, N_{Re} = 2.0, N_F = 0.1, \Pr = 6.2, Nc = 0.1$

ε	M	$f''(0)$	$-\theta'(0)$	$-s'(0)$
1.0	0.0	0.00000	0.71876	0.79071
	0.1	1.26872	0.720231	0.94423
	0.2	2.40418	0.72643	1.07013
2.0	0.0	2.78722	0.74456	1.13945
	0.1	3.71957	0.73228	1.28645
	0.2	4.76637	0.72977	1.43178

7. CONCLUSIONS

The laminar stagnation point nanofluid flow toward an exponential stretching sheet has been investigated. The analysis is offered to the individual effects of Nb, Nt and Ec whereas the combined effects of M and ε on the dimensionless temperature, velocity, and nanoparticle concentration profiles as well as on $f''(0), -\theta'(0)$ and $-s'(0)$. The brief conclusions of the analysis can be summarized as follows:

a) The non-dimensional velocity increases with , Nt, M, ε and Ec.

b) The dimensionless temperature at the surface increases with increasing Nb, Nt and Ec but decreases with increasing ε. However, the dimensionless temperature at the surface increases with increasing M when $\varepsilon = 2$ and decreases with increasing M when $\varepsilon = 1$.

c) The dimensionless surface concentration reduces with increasing Nb, M, ε and Ec but enhances with increasing Nt.

d) The increment of reduced skin friction coefficient occurs for the higher values of Nb, Nt, M, ε and Ec.

e) The enhancement in rate of heat transfer occurs for the higher values of ε and lower values of Nb, Nt and Ec.

f) The electrification parameter M enhances the heat transfer rate when both the

g) The dimensionless mass transfer coefficient reduced Sherwood number is an increasing function of Nb, M, ε and Ec and while it is a decreasing function of Nt.

REFERENCES

1. **Aghamajidi, M., Yazdi, M. E., Dinarvand, S. and Pop, I. (2018)**. Tiwari-Das nanofluid model for magnetohydrodynamics (MHD) natural convective flow of a nanofluid adjacent to a spinning down-pointing vertical cone, Propulsion and Power Research; 7(1):78-90.
2. **Alblawi, A., Malik, M. Y., Nadeem, S. and Abbas, N. (2019)**. Buongiorno's nanofluid model over a curved exponentially stretching surface, Processes, 7, 665; doi:10.3390/pr7100665.
3. **Alsaedi, A., Awais, M. and T. Hayat, (2012)**. Effects of heat generation/absorption on stagnation point flow of nanofluid over a surface with convective boundary conditions, Commun Nonlinear Sci Numer Simulat 17, 4210- 4223.
4. **Anuar N. S. and Bachok, N. (2016)**. Blasius and Sakiadis Problems in Nanofluids using Buongiorno Model and Thermophysical Properties of Nanoliquids, European International Journal of Science and Technology, Vol.5, No. 4, 65-81.
5. **Bachok, N., Ishak, A. and Pop, I. (2012a)**. Boundary layer stagnation-point flow and heat transfer over an exponentially stretching/shrinking sheet in a nanofluid, International Journal of Heat and Mass Transfer 55, 8122-8128.
6. **Bachok, N., Ishak, A. and Pop, I. (2012b)**. Unsteady boundary layer flow and heat transfer of a nanofluid over a permeable stretching/shrinking sheet, International Journal of Heat and Mass Transfer, 55, 2102-2109.
7. **Bhattacharyya, K. and Layek, G.C. (2014)**. Magnetohydrodynamic boundary layer flow of nanofluid over an exponentially stretching permeable sheet, vol. 2014, Article ID 592536, 12 pages.
8. **Magyari, E. and Keller, B. (1999)**. Heat and mass transfer in the boundary layers on an exponentially stretching continuous surface, Journal of Physics D, vol. 32, no.5, pp. 577-585.
9. **Malvandi, A., Hedayati, F. and Domairry, G. (2013)**. Stagnation point flow of a nanofluid toward an exponentially stretching sheet with non-uniform heat generation/absorption, Journal of Thermodynamics, vol. 2013, Article ID 764827, 12 pages
10. **Nadeem S. and Lee, C. (2012)**. Boundary layer flow of nanofluid over an exponentially stretching surface, Nanoscale Research Letters, vol. 7, article 94, pp. 1-15.

11. **Narender, G. and Sarma, G. S. (2019)**. The impact of radiation effect on MHD stagnation-point flow of a nanofluid over an exponentially stretching sheet in the presence of chemical reaction, Int. J. of Applied Mechanics and Engineering, vol.24, No.4, pp.125-139.
12. **Rahman, M. M. (2014)**. Locally similar solutions for hydromagnetic and thermal slip flow boundary layers over a flat plate with variable fluid properties and convective surface boundary condition, Meccanica 46: 1127-1143, DOI 10.1007/s11012-010-9372-2.
13. **Rehman, F. U., Nadeem, S., Rehman, H. U. and Haq, R. U. (2018)**.
14. Thermophysical analysis for three-dimensional MHD stagnation-point flow of nano-material influenced by an exponential stretching surface, Results in Physics 8, 316-323.
15. **Sandeep, N. and Jagadish Kumar, M. S. (2016)**. Heat and Mass Transfer in Nanofluid Flow over an Inclined Stretching Sheet with Volume Fraction of Dust and Nanoparticles, Journal of Applied Fluid Mechanics, Vol. 9, No. 5, pp. 2205-2215.
16. **Sandeep, N., Sulochana, C. and Rushi Kumar, B. (2016)**. Unsteady MHD radiative flow and heat transfer of a dusty nanofluid over an exponentially stretching surface, Engineering Science and Technology, an International Journal 19, 227-240.
17. **Wahid, N. S., Arifin, N. Md., Khashi'ie, N. S. and Pop, I. (2021)**. Hybrid nanofluid slip flow over an exponentially stretching/shrinking permeable sheet with heat generation, Mathematics, volume 9, issue 1, 30.

.